Investigation of Non-Punch-Through IGBTs with different trench designs

V. Kartal, W. Gerlach

Institute of Microelectronics and Solid State Electronics
TU Berlin, Jebensstraße 1, 10623 Berlin, Germany

Abstract

The influence of the trench design on the static and dynamic behavior of high voltage non-punch-through-IGBTs is numerically examined using the program „MEDICI". Moreover an analytical model is presented describing the dependence of the carrier distribution in the trench corridor of the NPT-trench IGBT.

1. Introduction

An important aspect of the optimization of an IGBT is the reduction of its static on-state losses. In the case of high voltage NPT-trench IGBT devices, the voltage drop occurs in the trench corridor and in the n^--base between the trench corridor and the p^+-anode. In order to optimize the on-state behavior, it is necessary to understand the dependence of the voltage drop in the trench corridor on the trench geometry. This can be calculated if the current and carrier distribution in the corridor are known.

2. Analytical Model

This paper presents an analytical model which describes the dependence of the carrier distribution in the trench corridor on the NPT-trench IGBT. This dependence is shown to be a direct result of the two dimensional current flow in the proximity of the p^+-collector.
As can be seen in fig.1 and fig.2, the electron and hole currents enter the trench corridor at $y = -a$. First they flow homogeneously in the y-direction in the trench corridor. The reverse biased cathode-base junction acts as a collector for the holes due to the direction of the electric field $\vec{E}$ in its space charge region (SCR). In contrast to its action on holes, the electric field in the SCR of the cathode-base junction prevents electrons from entering into the p^+-cathode.
Therefore the electron current bends off laterally in the x-direction and flows off over the MOS-channel (part II).
Fig.3 shows the electron and hole current in the trench corridor section along the line d-a. For the analytical model, the electron and hole current distribution

shown in fig.4 is assumed. The model is developed under the following assumptions:
The recombination is neglected. In the basis there is high injection and quasi neutrality. The hole current is constant in part I and in part II. The electron current drops linearly in part II while it is constant in part I.
The total current density $J_{tot} = J_p + J_n$ is given by the ambipolar current relations:

$$J_n(y) = \frac{b}{b+1} \cdot J_{tot} + q \cdot D_A \cdot \frac{dn}{dy} \quad (1.1)$$

$$J_p(y) = \frac{1}{b+1} \cdot J_{tot} - q \cdot D_A \cdot \frac{dn}{dy} \quad (1.2)$$

The carrier gradient in part I can be determined by solving the equation (1.1) and (1.2)

$$\frac{dn}{dy} = \frac{J_n^* - b \cdot J_p^*}{(b+1) \cdot q \cdot D} - \frac{J_n^*}{(b+1) \cdot q \cdot D_A} \cdot \frac{y}{d} \quad (1.3)$$

The integration of the equation (1.3) yields to the excess carrier concentration

$$n(y) = \frac{b \cdot J_p^*}{(b+1) \cdot q \cdot D_A} \cdot d + \left(\frac{J_n^* - b \cdot J_p^*}{(b+1) \cdot q \cdot D_A}\right) \cdot y - \frac{J_n^*}{(b+1) \cdot q \cdot D_A} \cdot \frac{y^2}{d} \quad (1.4)$$

for part I and

$$n(y) = \frac{b \cdot J_p^*}{(b+1) \cdot q \cdot D_A} \cdot d + \left(\frac{J_n^*}{(b+1) \cdot q \cdot D_A}\right) \cdot y - \frac{b \cdot J_p^*}{(b+1) \cdot q \cdot D_A} \cdot y \quad (1.5)$$

for part II.
Fig.7 shows the carrier distribution in the trench corridor. As can be seen the analytical model describes the carrier distribution in the trench corridor well.

3. Simulation results

3.1. Variation of trench depth

The influence of the trench design on the static and dynamic behavior of high voltage non-punch-through-IGBTs is simulated using the program „MEDICI". Fig.5 shows the structure, which has been varied in its trench depth. In fig.6 the carrier distribution of the IGBTs can be seen. Fig.6 shows, that a better conductivity modulation of the n-basis results from a greater depth of the trench corridor.
The 2D-plots illustrate that the voltage drop along the trench corridor rises when the trench depth is increased. This compensates for the decrease in voltage drop over the rest of the drift region (fig.8).

3.2. Variation of trench design

In order to reduce the switching losses and to optimize the switching time of the IGBT, the width and shape of the gate oxide in the trench bottom is varied. The main goal is to reduce the miller capacitance. Fig.9 shows the structures of the different IGBTs examined. Fig.10 shows the hole distribution in a solid line for the VG, in a dotted line for the TG and in a broken line for SG. Even though the accumulation layer at the gate bottom is weakened in the VG- and SG-type IGBT, this does not have a significant influence on the carrier concentration in the n-basis as shown in fig.10 [4], contrary to the assumption in [3]. However, the reduced miller capacitance influences the switching time. Fig.11 and fig.12 show a reduction in the turn-off and turn-on time. The turn-off losses are also drastically reduced.

4. References

[1] Kitagawa, M. Omura, I. Hasegawa, S. Tomoki, I. Nakagawa, A. IEDM Washington, Dezember 5-8, 1993.

[2] Amaratunga, A.J. Udrea, F. IEEE Transactions on Electron Devices, Juli 1995. Vol. 42, Nr.7.

[3] Omura, I. Ogura, T. Sugiyama, K. Ohashi, H. ISPSD Weimar, May 26-29, 1997.

[4] Schönauer, T. Kartal, V. Gerlach, W. ISPS'96 3rd. Prag, September 11-13, 1996

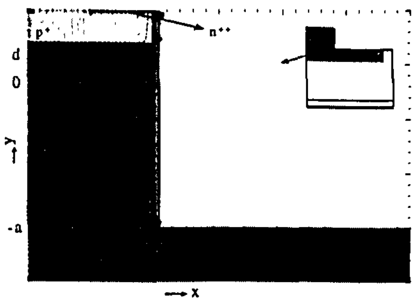

Fig.1 2D-Electron current vectors in trench corridor

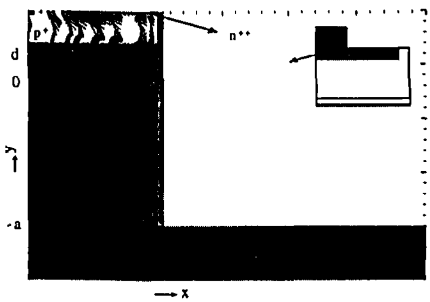

Fig.2 2D-Hole current vectors in trench corridor

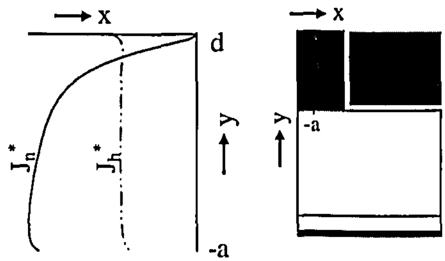

Fig.3 Hole- and electron current density in trench corridor (real)

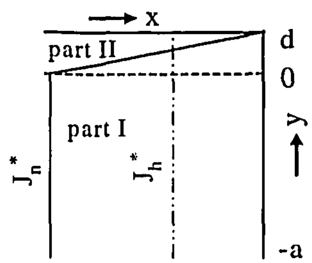

Fig.4 Hole- and electron current density in trench corridor (symbolically)

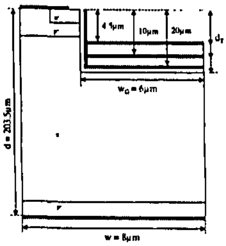

Fig.5 IGBT-Structure

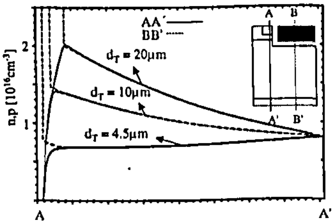

Fig.6 Carrier distribution with different trench depth d_T.

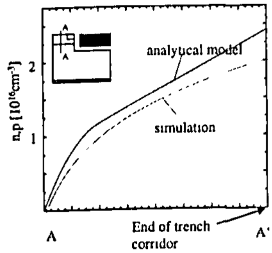

Fig.7 Carrier distribution in the trench corridor

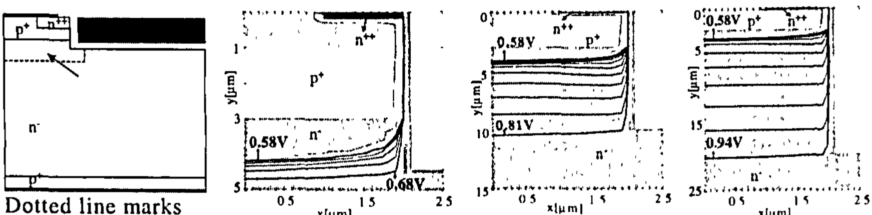

Dotted line marks area of contours of potential

$d_T = 4.5\mu m$ $d_T = 10\mu m$ $d_T = 20\mu m$

Fig.8 Contours of potential in the trench corridor of IGBTs with different trench depth

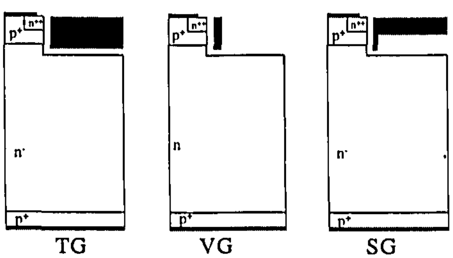

Fig.9 The structure of different IGBTs

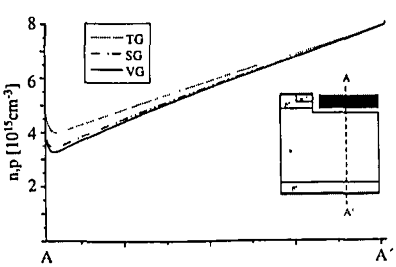

Fig.10 Hole distribution of different trench structure

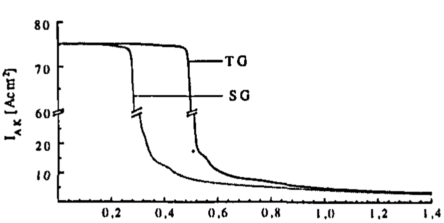

Fig.11 Transient turn-off characteristics for the TG- and SG-IGBT

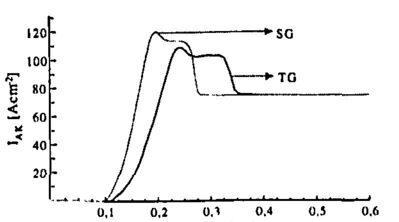

Fig.12 Transient turn-on characteristics for the TG- and SG-IGBT